Dengue epidemics and human mobility

D. H. Barmak, C. O. Dorso, M. Otero, and H. G. Solari
Departamento de Física, Facultad de Ciencias Exactas y Naturales, Universidad de Buenos Aires and IFIBA, CONICET, Pabellón I, Ciudad Universitaria, Nuñez, 1428 *Buenos Aires, Argentina*
(Received 18 February 2011; revised manuscript received 2 May 2011; published 1 July 2011)

In this work we explore the effects of human mobility on the dispersion of a vector borne disease. We combine an already presented stochastic model for dengue with a simple representation of the daily motion of humans on a schematic city of 20 × 20 blocks with 100 inhabitants in each block. The pattern of motion of the individuals is described in terms of complex networks in which links connect different blocks and the link length distribution is in accordance with recent findings on human mobility. It is shown that human mobility can turn out to be the main driving force of the disease dispersal.

DOI: 10.1103/PhysRevE.84.011901 PACS number(s): 87.10.Mn, 87.23.Ge, 05.10.Gg

I. INTRODUCTION

Dengue fever is a vector borne disease produced by a *flavivirus* of the family *flaviviridae* [1]. It is found in tropical and subtropical regions around the world, predominantly in urban and semiurban areas. Dengue hemorrhagic fever (DHF) [2], a potentially lethal complication, was first recognized in the 1950s during dengue epidemics in the Philippines and Thailand and nowadays affects most Asian countries and has become a leading cause of hospitalization and death among children in the region.

There are four distinct, but closely related, serotypes of the virus that cause dengue: DEN1, DEN2, DEN3, and DEN4. Recovery from infection by one provides lifelong immunity against that serotype but confers only partial and transient protection against subsequent infection by the other three serotypes. There is good evidence that sequential infection with different serotypes increases the risk of developing DHF. Recently, the number of countries affected by this epidemic has increased and severe forms have become more frequent. The main vectors of dengue are *Aedes aegypti* and *Aedes albopictus*.

This problem attracts the attention of researchers in different fields from biologists to physicists [3]. The research aimed at producing dengue models for public policy use began with Newton and Reiter [4] who introduced a minimal model for dengue in the form of a set of ordinary differential equations (ODE) for the human population disaggregated in susceptible, exposed, infected, and recovered compartments. The mosquito population was not modeled in this early work. A different starting point was taken by Focks *et al*. [5,6] that began by describing mosquito populations in a computer framework named Dynamic Table Model, where later the human population (as well as the disease) was introduced [7].

Newton and Reiter's model (NR) favors economy of resources and mathematical accessibility; in contrast, Fock's model emphasizes realism. These models represent in dengue two contrasting compromises in the standard trade-off in modeling. A third starting point has been recently added. Otero and Solari (OS) developed a dengue model [8] which includes the evolution of the mosquito population [9,10] and is spatially explicit. This last model is somewhat in between Fock's and NR as it is formulated as a state-dependent Poisson model with exponentially distributed times.

ODE models have received most of the attention. Some of the works explore variability of vector population [11], human population [12], the effects of hypothetical vertical transmission of dengue in vectors [13], seasonality [14], and age structure [15] as well as incomplete gamma distributions for the incubation and infectious times [16]. Comparison with real epidemics has shown that there is a need to consider the spatial heterogeneity as well [17].

In a previous work [18] we have developed a dengue model which includes the evolution of the mosquito population and is spatially explicit. In that work the spatial spread of the infection was driven by the flights of mosquitoes that gave rise to a diffusion process. In it we analyzed the evolution of dengue infection in a city of 20 × 20 blocks with 100 individuals in each one. This population was fixed throughout the calculation and no mobility of the individuals was allowed.

As such, in that model, the spatial evolution of the dengue infection was only driven by the flight of mosquitoes as the mobility of humans was not included. It is usually recognized that human mobility is not only necessary to be included in human infection spread models, but that it might be the main source of the dynamics behind spatiotemporal phenomena on geographic scales (i.e., the spread of infection from city to city due to people flying long distances by plane). It is thus very important to address the problem of the mobility of humans and incorporate it into the models to be able to make more reliable predictions, and then, to be able to propose effective public policies against the dispersal of a known or emerging disease.

Including the mobility of the human population in a model is not an easy task given the complexity of human behavior. The first problem to address is the technical and ethical difficulties that arise when trying to get information about the mobility of humans. There are many databases from which this data could be inferred, such as the ones associated to cellular phone networks, credit cards, hotel reservations, flight reservation databases, etc. But as almost all of them are private, most researchers do not have access to them. Moreover, even if we did have them, mixing this diversified information together to get a human mobility model is a hard task by itself. Aside from these particular difficulties, there is an intrinsic bias on the databases if we are going to use them for diseases spread, because it is reasonable to think that human behavior will change or adapt in the presence of social awareness of a disease

TABLE I. Human state according to the cycle day of the infection.

Cycle day (days)	Human state
d_0	The virus is transmitted by the bite of an infected mosquito.
$d_0 + \tau_E(h)$	The human enters the infective stage.
$d_0 + \tau_E(h) + j$	The human is infective and is able to transmit the virus with probability $p_{hm}(j)$, if bitten by a susceptible mosquito.
$d_0 + \tau_E(h) + \tau_i$	The human enters the recovered stage. No longer transmits dengue.

[19–28], and the inferences made on these databases cannot take that into account. Moreover, there can be a social bias because not everyone may use credit cards, go to hotels, etc.

Whether it is necessary to have detailed information on the movements of each individual to build up a model, or if it is only needed a coarse grain statistics of the mobility as a whole is an open question which still has to be answered [29]. Several works tackle the issue of the correct description of the mobility of human beings, relying on different methods and databases [30–37].

As most works focusing on this topic analyze the effect of human mobility in human-human transmitted diseases [21,22,24–28,38–40], but not in vector borne ones [29,41,42], in the present work we show a variation of our previous dengue model which not only includes the flight of the mosquitoes but also the mobility of the human beings. We then show the key differences in the results between both our models and conclude on the actual impact of human behavior on dengue.

In Sec. II we describe the characteristics of the epidemiological model we use in this work encompassing the dynamics of the virus for humans and mosquitoes and the dispersal dynamics for each. In Sec. III we present the results of our numerical investigations which include the analysis of the size and time evolution of the epidemics and the morphological properties of the patterns of spatial distributions of the infections for different mobility patterns and for different densities of mosquitoes. Finally, conclusions are drawn in Sec. IV.

II. THE EPIDEMIOLOGICAL MODEL

There are four ingredients in this model: the epidemiological dynamics of the infected mosquitoes, the epidemiological dynamics of the infected humans, and the mobility patterns of the individuals and the mosquitoes. Each of these elements will be discussed in the following sections.

A. Mosquitoes

The dengue virus does not have any effect on the vector; as such, *Aedes aegypti* populations are independent of the presence of the virus. In the present model mosquito populations are produced by the *Aedes aegypti* model [10] with spatial resolution of one block using climatic data tuned to Buenos Aires, a temperate city where dengue circulated in the summer season 2008–2009 [43]. The urban unit of the city is the block, approximately a square of (100 × 100 m). Because of the temperate climate the houses are not open as is often the case in tropical areas. Mosquitoes develop in the center of the block, which often presents vegetation, and then communicate to the houses of the block. The model then assumes that mosquitoes belong to the block and not to the houses and they blood feed with equal probability in any human resident in the block. *Aedes aegypti* is assumed to disperse seeking for places to lay eggs. The mosquito population, number of bites per day, dispersal flights, and adult mortality information per block are obtained from the mosquito model [10]. The time step of the model has been fixed at one day.

The virus might enter the mosquito when it bites a viremic human. The virus is actually transmitted from the infected human to the susceptible mosquito with a probability $p_{hm}(j)$, dependent on the day j in the infectious cycle of the human bitten.

The cycle continues with the reproduction of the virus within the mosquito (extrinsic period) that lasts τ_m days. After this reproduction period the mosquito becomes infectious and

TABLE II. Levy-flight distribution parameters.

	r_0 (m)	β	κ (m)
1	200	1.65	1500
2	200	2.	1500
3	200	3.	1500
4	200	4.	1500

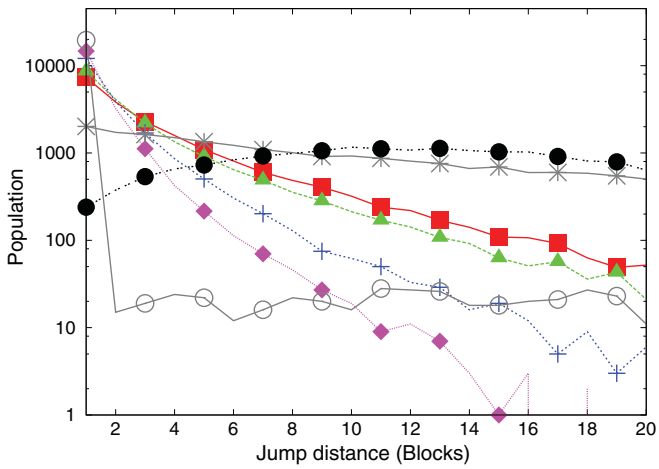

FIG. 1. (Color online) Distribution of jump length for different mobility patterns. $R1$ (solid circles), $R2$ (open circles), Levy flights with $\beta = 1.65$ (solid squares), $\beta = 2$ (solid triangles), $\beta = 3$ (crosses), and $\beta = 4$ (solid diamonds). As a comparison, the Levy flight with parameters from the Barabasi distribution is shown with asterisks [31].

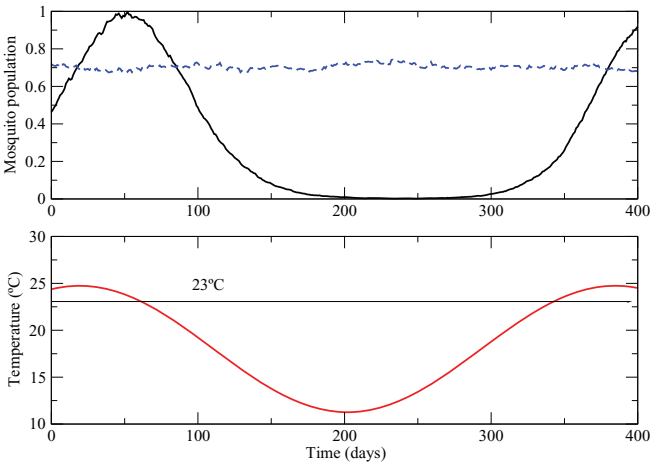

FIG. 2. (Color online) Top: Normalized mosquito population for constant temperature (dashed) and seasonal variation (full). Bottom: Temperature profile for constant and seasonal variation, as described using the model as seen in [10]. Day 0 is set at the 1st of January.

transmits the virus when it bites with a probability p_{mh}. The mosquito follows a cycle, susceptible, exposed, infected (SEI), and does not recover. Eventually mosquitoes die with a daily mortality of 0.09 [9]. The adult female mosquito population as produced by the *Aedes aegypti* simulation is then split into susceptible, τ_m stages of exposed and one

TABLE III. Mean shortest path and clusterization for the human mobility networks.

Network	l (Blocks)	C
$R1$(uniform)	1.779	0.220
Levy ($\beta = 1.65$)	2.006	0.286
Levy ($\beta = 2$)	2.112	0.303
Levy ($\beta = 3$)	2.532	0.349
Levy ($\beta = 4$)	3.092	0.380
$R2$	3.884	0.014

infective compartment according to their interaction with the viremic human population and the number of days elapsed since acquiring the virus. The mosquito population of each block is not fixed, but instead mosquitoes move around in terms of a simple diffusion process, as described in [10].

B. Humans

The evolution of the disease in one individual human, h, evolves as follows.

In Table I, $\tau_E(h)$ stands for the intrinsic incubation time, and τ_i is the viremic time of each individual. The cycle in the human being is then of the form susceptible, exposed, infected, recovered (SEIR). Each human has its own value of τ_E which is assigned according to Nishiura's experimental distribution [44].

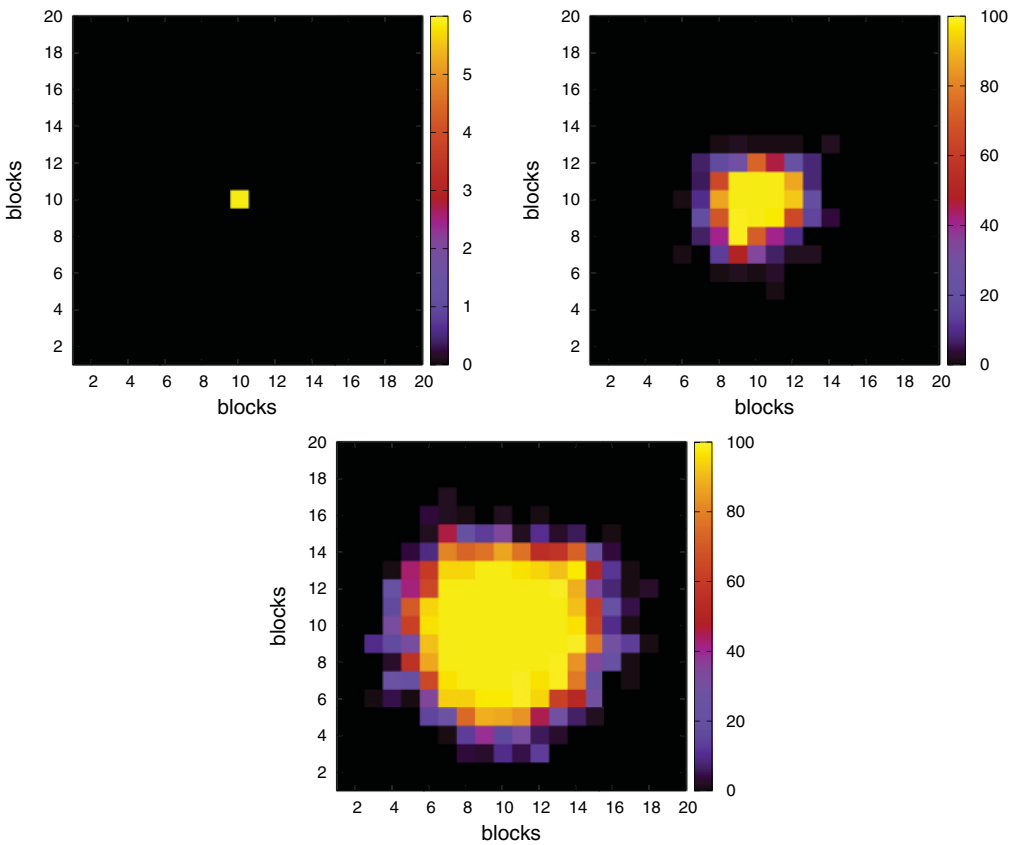

FIG. 3. (Color online) Spatial distribution of the number of recovered individuals for three times, namely, 25, 81, and 173 days for the case of a dengue epidemic driven only by the dispersal of mosquitoes. It can be seen that the pattern corresponds to a diffusive process and the evolution is highly symmetric.

As mentioned above, our analysis of the time evolution of dengue fever is performed on a schematic city in which the basic unit is the block and in each block a human population of 100 individuals is placed. The human population of each block is not fixed in the present work. In order to describe the patterns of mobility of the humans we have adopted the following schematic model: 50% of the population of each block is randomly selected to be mobile, while the other 50% is considered to remain in its original block during the whole analysis. Each mobile individual is assumed to stay 2/3 of the day in its original block, while the other 1/3 of the day she/he will stay in a randomly assigned block according to patterns described in the following. In each case, each of the mobile individuals is assigned a fixed destination to which it returns everyday. At the end of the day individuals return to their original block. This random assignment is performed according to certain rules that will characterize the mobility pattern. Following recent works on human mobility, referred to in the Introduction, we require that the movement of each individual (a) should be highly predictable [45] and (b) the distribution of the lengths of the displacements of the human should follow a truncated Levy distribution [31] which reads

$$P(r) \propto (r + r_0)^{-\beta} \exp(-r/\kappa), \tag{1}$$

with $P(r)$ the probability of a human traveling a distance, where r_0, β, and κ are parameters that characterize the distribution. In this work we have used the parameters described in Table II.

Such a pattern of mobility of the humans is accomplished by building a network with 50 links starting in each block. The length of the link is distributed according to the proposed length distribution and the final block is chosen at random from those which can be reached by the link. Each link is assigned to a mobile human at the start of the simulation. The distribution of jump sizes for each type of underlying network is shown in Fig. 1. In order to have reference mobility networks we have also analyzed the case in which the end points of the links are completely random (uniform distribution) which we call $R1$. We have also investigated the case in which only one individual per block performs a random jump, while the rest of the mobile individuals in the block visit only their neighboring blocks ($R2$).

Once the set of parameters is fixed, different underlying networks are generated and a set of evolutions (typically a couple of thousand events) is performed for such arrangements.

C. The networks

The networks built according to the above-mentioned prescription can be analyzed in order to unveil their "small world properties." We have found it interesting to study the geodesic path, i.e., the average minimum path between all the

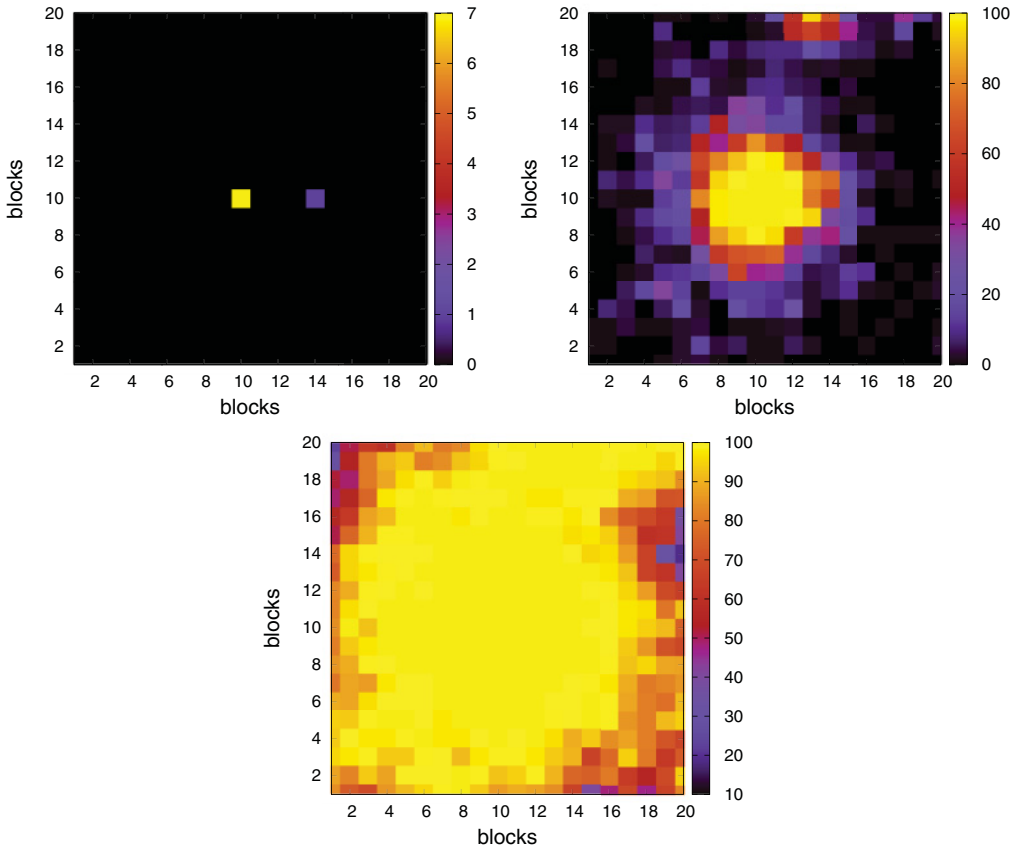

FIG. 4. (Color online) For the same times as in Fig. 3, the spatial distribution of recovered individuals when their mobility is modeled by a truncated Levy flight with $\beta = 3$. It can be seen that, at variance with Fig. 3 the pattern is asymmetrical; moreover, the evolution is faster and it can be seen that at $t = 81$ days a second focus is present.

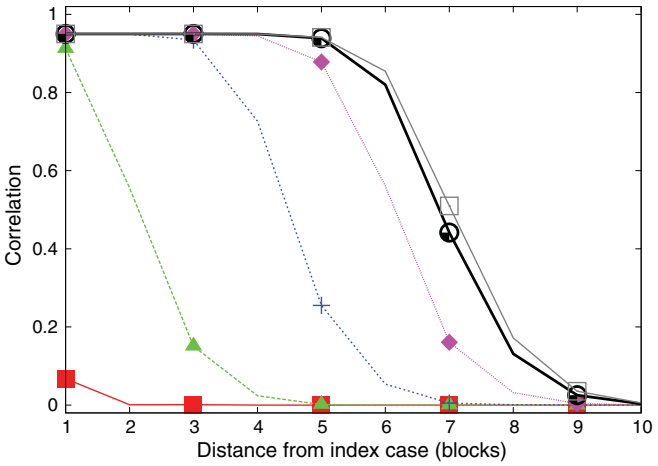

FIG. 5. (Color online) Radial correlation function as defined in the text for the case in which the spatial evolution of the epidemics is driven by the dispersal of mosquitoes only. Solid squares (red): $t = 25$ days; solid triangles (green): $t = 57$ days; crosses (blue): $t = 89$ days; diamond (violet): $t = 121$ days: open circles (black): $t = 153$ days; open squares (gray) $t = 189$ days. The pattern of variation is quite regular as expected for a diffusive case.

cells.

$$l = \frac{1}{n(n-1)} \sum_{i,j \neq i} d_{ij}, \tag{2}$$

with d_{ij} the minimum path between cells i and j, and n the total number of nodes. The minimum path is defined as the minimum number of links that are to be traversed in order to travel from the original block to the destiny block. Therefore, we see that it is a simple average over all the possible pairs of blocks in the system of the minimum distance between each pair.

Another interesting quantity to explore the characteristics of a network is the so-called clustering. One of the usual

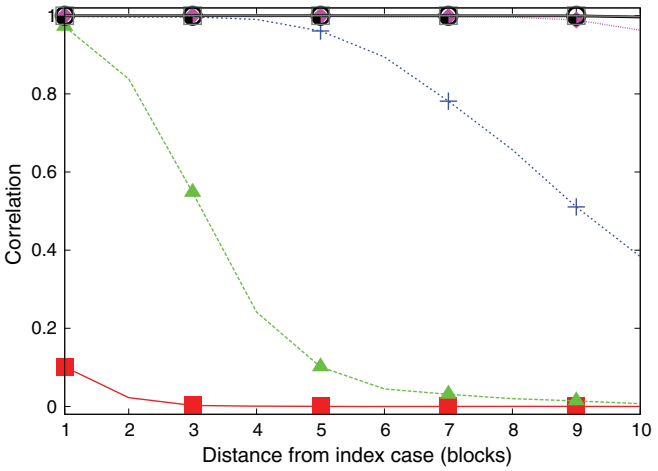

FIG. 6. (Color online) Radial correlation function as defined in the text for the case in which the humans move with the Levy-flight ($\beta = 3$) distribution. Solid squares (red): $t = 25$ days; solid triangles (green): $t = 57$ days; crosses (blue): $t = 89$ days; diamond (violet): $t = 121$ days; open circles (black): $t = 153$ days; and open squares (gray): $t = 189$ days.

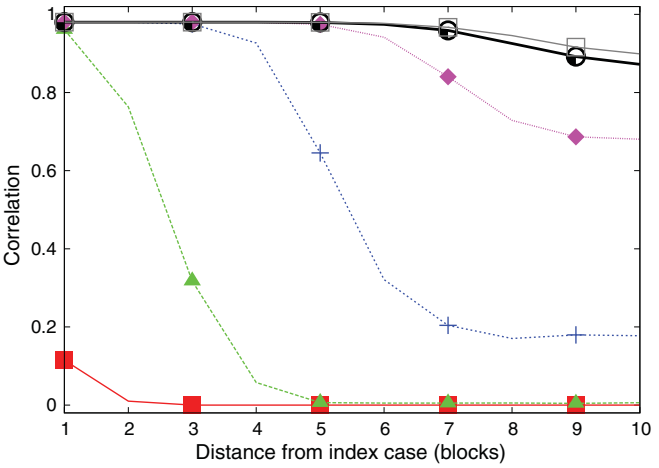

FIG. 7. (Color online) Radial correlation function as defined in the text for the case in which only one human per block moves at random, and the rest move to neighboring blocks ($R2$). Solid squares (red): $t = 25$ days; solid triangles (green): $t = 57$ days; crosses (blue): $t = 89$ days; diamond (violet): $t = 121$ days; open circles (black): $t = 153$ days; and open squares (gray): $t = 189$ days.

definitions of this quantity is as follows: Given a node i with k_i nearest neighbors we define c_i as

$$c_i = \frac{2}{k_i(k_i-1)} \times (\text{number of links between nearest neighbors}), \tag{3}$$

$$C = \frac{1}{n} \sum_i c_i. \tag{4}$$

In Table III we show the results of such a calculation.

We can see from Table I that the mean shortest path attains a minimum for the completely random pattern of links and grows as this pattern is replaced by the ones generated by the

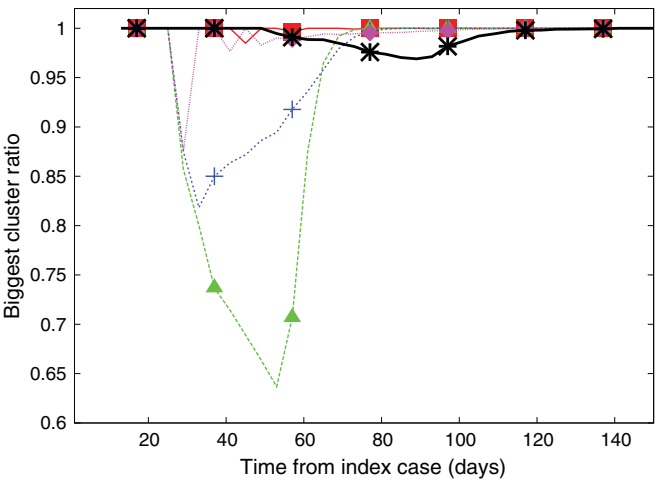

FIG. 8. (Color online) Ratio between the size of the biggest cluster (in terms of the number of recovered humans) and the total number of recovered. Diffusive (red solid squares), $R1$ (green solid triangles), Levy ($\beta = 1.65$) (blue crosses), Levy ($\beta = 4$) (violet solid diamonds), and $R2$ (black asterisks).

Levy flights. We see that the broader the Levy flight, the larger the average minimum path, as expected.

III. NUMERICAL CALCULATIONS

We have implemented the above described method (the algorithm without human mobility has been fully described in [18]) and have performed extensive calculations for different initial conditions. The conditions are as follows: a rectangular city of 20×20 blocks, mosquito breeding site densities, different realizations of the underlying mobility networks, and different seasonal conditions.

The number of breeding sites (BS) per block or density of breeding sites explored in these calculations are 50, 100, 200, 300, and 400. Larger numbers of breeding sites are considered to be unrealistic for the system we have in mind, i.e., the city of Buenos Aires. The human population density and the size of the grid were chosen accordingly to the size and human density of the neighborhoods typically infested with *Aedes aegypti* in the city of Buenos Aires. Larger sizes would require the consideration of spatial heterogeneities of the human population and breeding site density. Moreover, larger numbers of breeding sites do not add new information to our calculations.

Another relevant condition that we have explored is the underlying mobility network. For each value of the breeding site densities, evolutions with different underlying networks were performed.

Finally, we have considered two different seasonal conditions: in Fig. 2 we show the population (top) and temperature (bottom) profiles. In the seasonless situation, the temperature remains fixed all along the evolution at 23 °C. In this case the mosquito population remains basically constant all along the evolution. In such a case the size of the epidemics is determined by the dynamics of the infection itself subject to the above-mentioned boundary conditions. If we adopt the average temperature time distribution of Buenos Aires (see Fig. 2 for details) the population of mosquitoes is a strongly time dependent one; the size of the epidemics might then be severely constrained. It has to be noted that an exposed human (index case) is introduced near the center of the grid, on January 1st.

In what follows we will focus on certain properties of the epidemic system that are relevant for the understanding of the characteristics of the time evolution. First we study the morphology of the evolving spatial structure of the epidemics. Then we study the final size and time span of the epidemics. Then we include the results of the analysis of a system in which

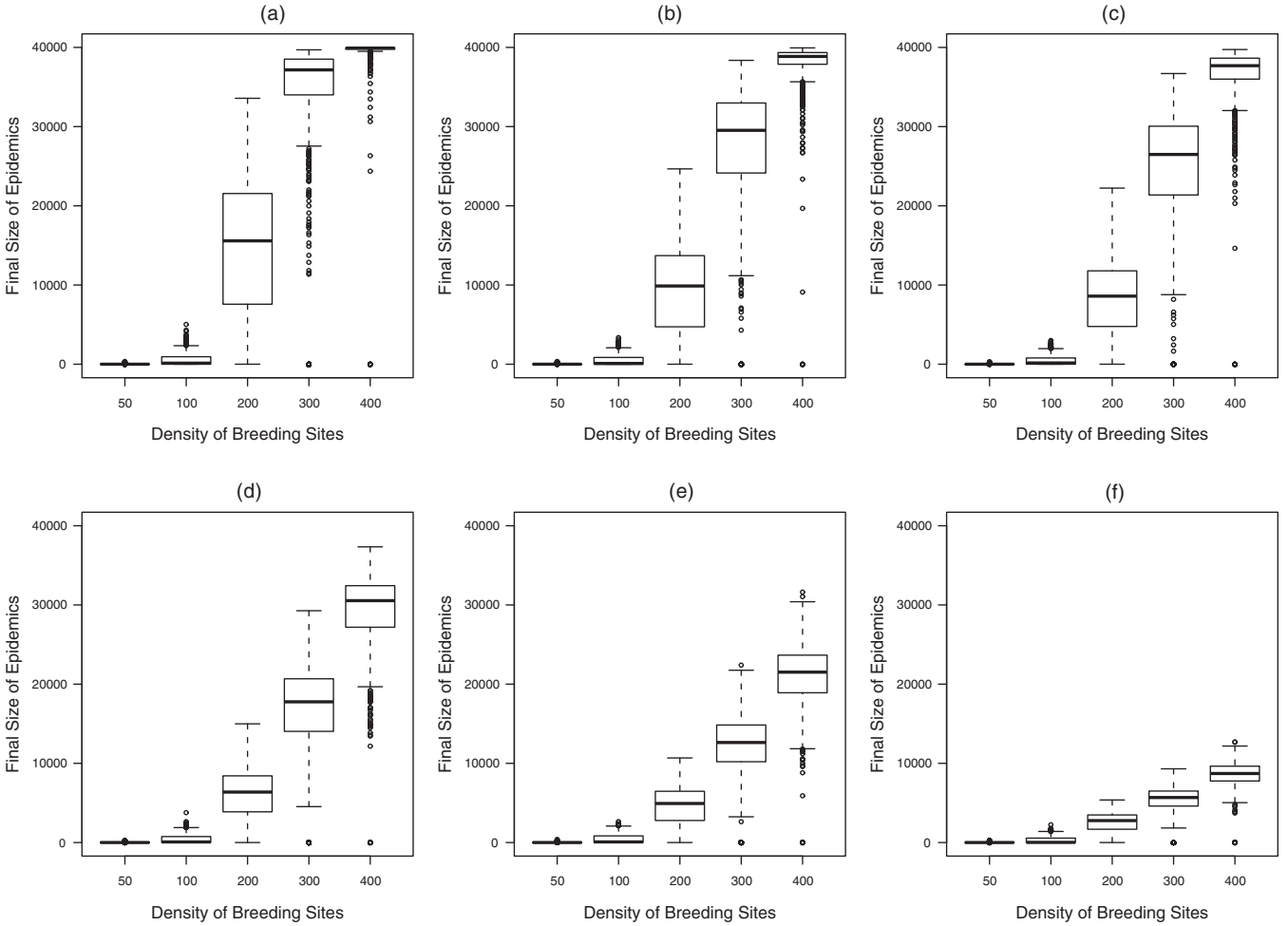

FIG. 9. Box-plot graphs of the final size of epidemics for different patterns of human mobility: (a) $R1$, (b) Levy ($\beta = 1.65$), (c) Levy ($\beta = 2$), (d) Levy ($\beta = 3$), (e) Levy ($\beta = 4$), and (f) no movement.

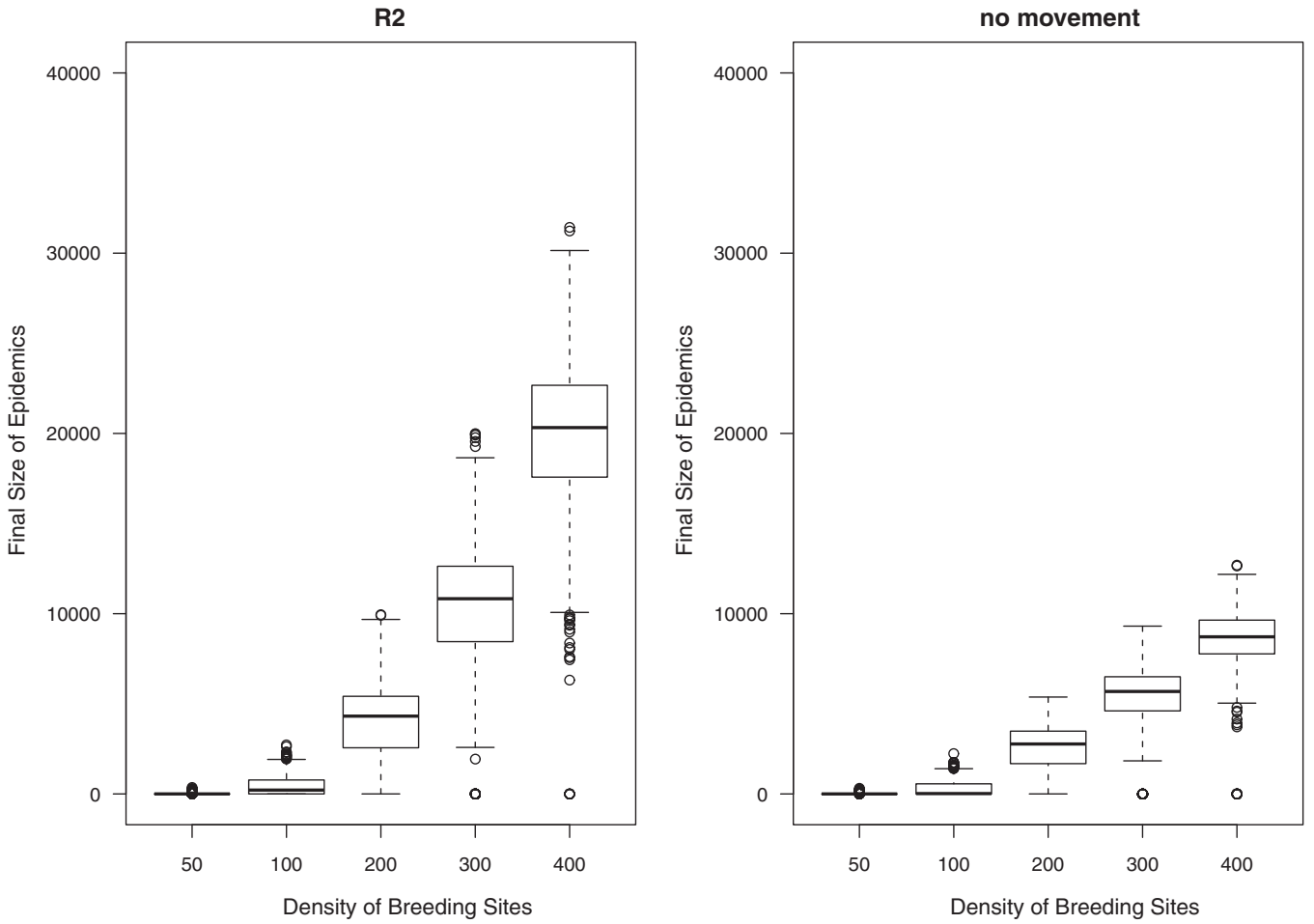

FIG. 10. Box-plot graphs of the final size of epidemics for different patterns of human mobility: (Left) $R2$ and (right) no human mobility.

the temperature is kept fixed at 23 °C. Finally, we study a new quantity that we name the *power* of the epidemics.

A. Morphology of the spatial structure of the epidemics

It is expected that human mobility increases the size and speed of the epidemics. This happens because each jump (shortcut) when executed by a virus carrying individual may induce the contagion of mosquitoes at the destination block and then generates a new dispersal center for the illness.

In Fig. 3 we show the density of recovered individuals at three relevant times for the case in which the dispersal of dengue is driven by the diffusion of mosquitoes only. It is seen that the population of recovered individuals displays a symmetrical pattern as expected from a simple diffusion process.

On the contrary, as seen in Fig. 4, the pattern for the case in which the human jumps follow a Levy-flight distribution is quite heterogeneous and it can be clearly seen that there is more than one dispersal center.

This observation can be made more quantitative if we calculate the radial correlation function defined as the probability of finding at least one infected (recovered) individual (calculated at the time at which all individuals have returned home) at a block such that it can be reached by a jump of length r from the place at which the initial infected individual was located (which in this case is a block close to the center of the city).

In what follows we show the result of calculating the radial correlation function for three typical cases, namely, for the mosquito-driven evolution, for the Levy-flight case with $\beta = 3$, and the case in which only one of the mobile individuals performs random jumps ($R2$).

From Figs. 5–7 it is clearly seen that in the presence of human mobility nearly all of the city can be reached by the epidemic in short times. On the one hand, in the case of mosquitoes only as a driving force, the correlation function displays patterns expected for a traveling wave front. In the other cases the wave front breaks early in the evolution and the correlation function is different from zero almost everywhere after a few days.

As we have seen in Figs. 3 and 4, the structure of the spatial density of, say, humans in state R is highly symmetric and compact for the case without human mobility. As human mobility (of the kind considered in this work) is incorporated, both the symmetry and the compactness are lost. In order to explore this behavior in a more quantitative way we define a cluster of recovered individuals in the following way. Given a block i we will call it an occupied block if at least one member of its original population is in the recovered state. A cluster (of size larger than one) is a set of occupied blocks in which all

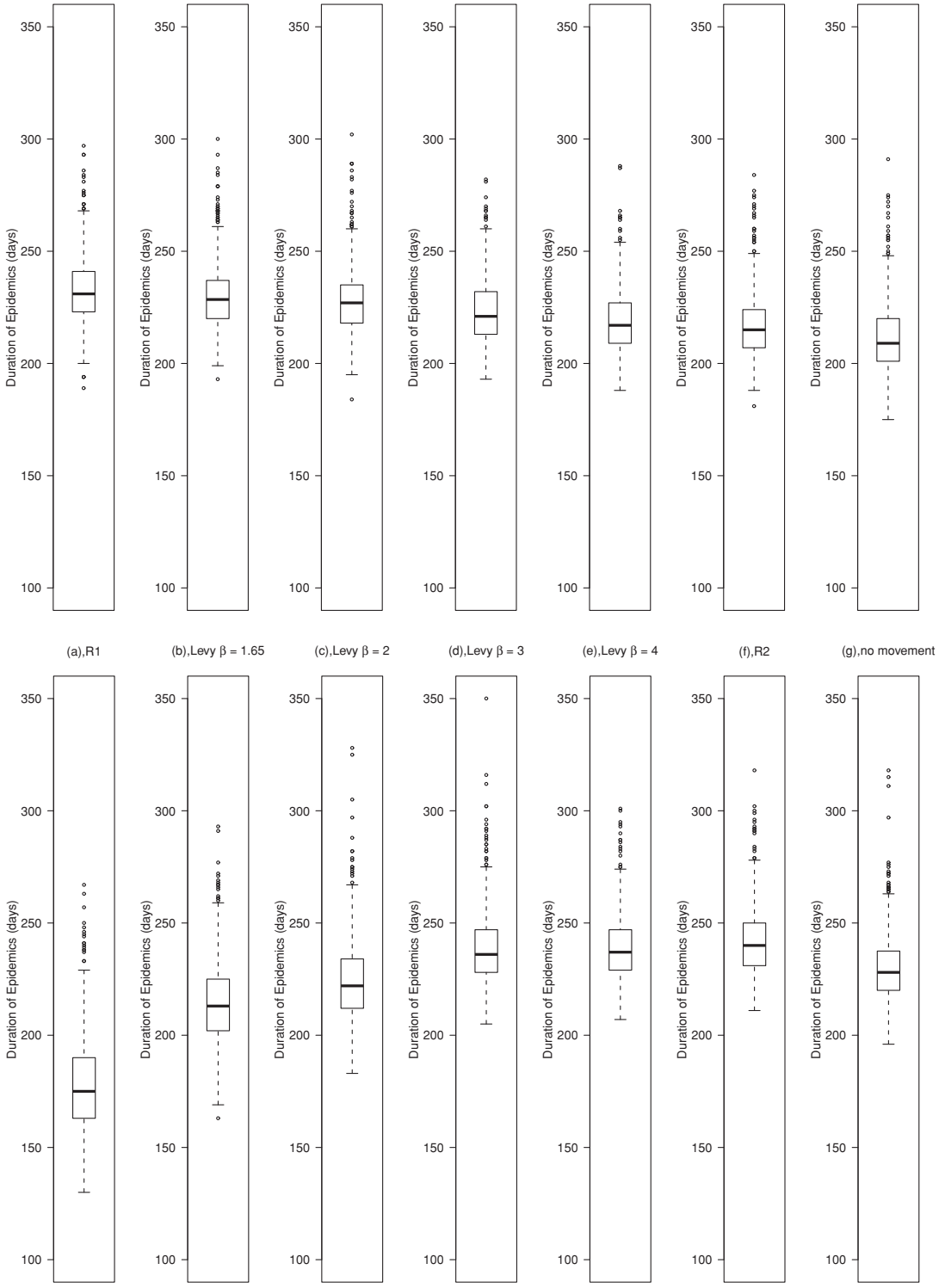

FIG. 11. Comparison of the duration of the epidemic outbreaks for the different patterns of human mobility, 200 breeding sites/ha (Top) and 400 breeding sites/ha (Bottom). (a) R1, (b) Levy ($\beta = 1.65$), (c) Levy ($\beta = 2$), (d) Levy ($\beta = 3$), (e) Levy ($\beta = 4$), (f) R2 and (g) no movement.

constituents have at least a nearest or second-nearest neighbor which belongs to the cluster. Then the block i will belong to the cluster if the following relation is satisfied:

$$i \in C \Longleftrightarrow \exists\ j \in C / i \text{ is a neighbor of } j. \qquad (5)$$

We define the mass of a cluster as the number of recovered individuals in the cluster. The results are displayed in Fig. 8.

It can be seen that for the case of simple diffusion all of the mass is concentrated in the biggest cluster. On the other hand, for the random ($R1$) case there is a time (around 50 days into

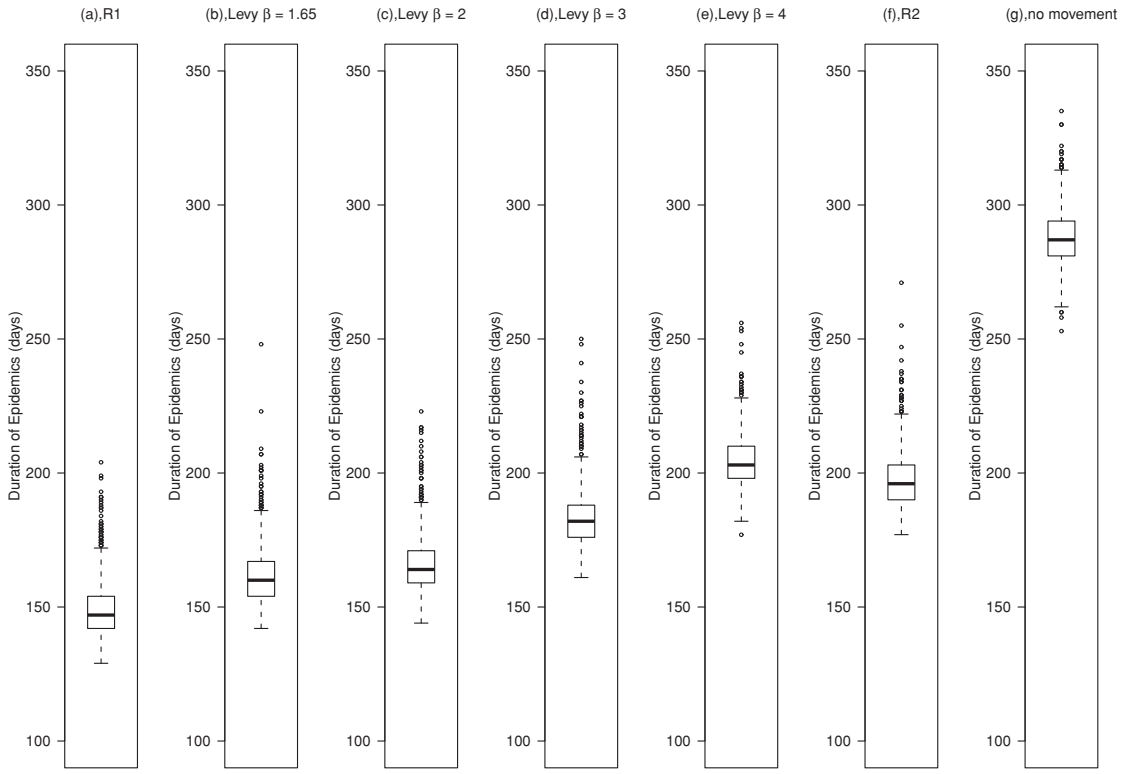

FIG. 12. Comparison of the duration of epidemics for the different patterns of human mobility at a constant temperature of 23 °C (400 breeding sites/ha). (a) R1, (b) Levy ($\beta = 1.65$), (c) Levy ($\beta = 2$), (d) Levy ($\beta = 3$), (e) Levy ($\beta = 4$), (f) R2 and (g) no movement.

the epidemic) at which only about 65% of the mass is in the biggest cluster. This is due to the emergence of secondary foci generated by infective humans who perform long jumps.

B. Sizes and time span of the epidemics

One of the main observables in this kind of problem is the final size of the epidemics. In what follows we show in Fig. 9 a comparison of the final size of the epidemics in terms of the box plots[1] corresponding to different densities of the breeding site densities for different patterns of human mobility. As described above, we have two limiting situations: (a) the case in which the moving humans perform jumps with completely random destinations and (f) the case in which the dispersal of the epidemics is only due to the diffusion of mosquitoes. In between we have the patterns related to the length of the jump given by a truncated Levy flight characterized by the different set of parameters shown in Table II, i.e., $\beta = 1.65$, 2, 3, and 4 (keep in mind the smaller β, the closer to the random case). The corresponding results are displayed in panels (b)–(e).

Finally, in Fig. 10 (left panel) we show the case in which only one of the mobile humans in each block performs a jump to a random destination while the others move to nearest neighbors. For the sake of completeness we show in the right panel the box plot corresponding to the mosquito-only-driven evolution.

It is immediate to see that the effect of human mobility for all the cases is to increase the final size of the epidemics with respect to the case in which the mosquito diffusion is the only driving force. Moreover, in the case of completely random (uniform) mobility and for the Levy flight with $\beta = 1.65$ we find that for the highest BS density proposed in this work, the epidemic spreads over the whole population.

Figure 11 shows the duration distribution of the epidemics as a function of the different patterns of human mobility and for two constant breeding site densities of 200 (top) and 400 BS/ha (bottom) . For 200 BS/ha (top) all box plots present a similar spread of data but a slight tendency to an increase of the median from right to left (from the case without mobility to the complete random pattern). Instead, for 400 BS/ha the tendency is to decrease from right to left. [This behavior will be properly discussed in terms of the power of the epidemics (see below).]

C. Behavior of the model at constant temperature

Figure 12 shows the duration distribution of the epidemics as a function of the different patterns of human mobility for a constant breeding site density of 400 BS/ha and a constant temperature of 23 °C. We see that the maximum duration of

[1]The box plot (or sometimes called box-and-whisker plot) is a simple method of displaying data, invented by Tukey [46]. To create the box-and-whisker plots, we drew a box with ends at the lower and upper quartiles and the statistical median as a horizontal line in the box. Then we extended the "whiskers" to the farthest points of the sample that were not outliers (i.e., that were within 1.5 times the interquartile range). Finally, for every point more than 1.5 times the interquartile range from the end of the box, a dot was drawn.

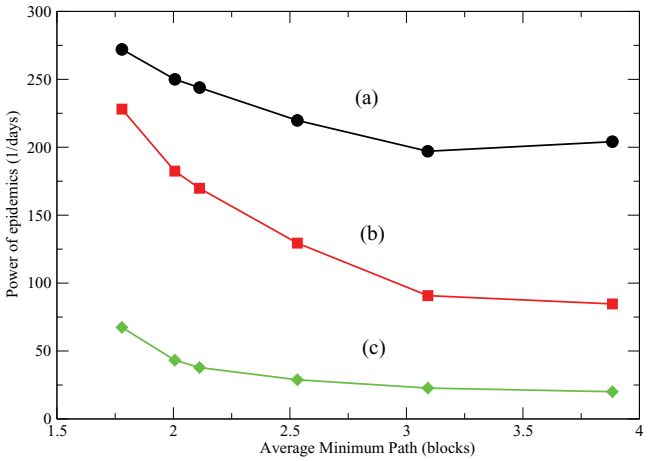

FIG. 13. (Color online) Comparison of the mean power of the epidemics for the different patterns of human mobility (from left to right: $R1$, Levy ($\beta = 1.65$), Levy ($\beta = 2$), Levy ($\beta = 3$), Levy ($\beta = 4$), and $R2$), characterized by the average minimum path for three conditions: (a) 400 BS/ha and a constant temperature of 23 °C, (b) 400 BS/ha, and (c) 200 BS/ha for seasonal variations of temperature.

the epidemic takes place for the case of no human mobility and it shortens as the patterns of mobility of the individuals tend to the completely random one. It is also interesting to note that in this case the epidemic involves the whole population in all cases.

D. Power of the epidemic

We define the mean power of the epidemic as the ratio between the median of the final size of the epidemic and the median of the duration of the epidemics.

$$P_m = \frac{M_{FS}}{M_\tau}. \tag{6}$$

Figure 13 shows the mean power for three conditions: (a) 400 BS/ha and a constant temperature of 23°C, (b) 400 BS/ha and seasonal variation of temperature, and (c) 200 BS/ha and seasonal variation of temperature. The P_m grows with broader jump length distributions and with higher BS densities. The case of 400 BS/ha is higher for constant temperatures than for seasonal variations of temperature. If we compare 400 and 200 BS/ha (for seasonal variations of temperature) we see the same increasing tendency of P_m with human mobility, but this value is higher for 400 BS/ha than for 200 BS/ha. (For the case of 400 BS/ha and constant T the increase of the power of the epidemic is a consequence of the reduction of its duration as the pattern of human mobility approaches the fully random case. At constant T all of the population gets infected. On the other hand, when the temperature is not fixed it severely constrains the mosquito population and then the increase in P_m is mainly due to the increase of the size of the infected population as the time span of the epidemics is only mildly dependent on the driving force of the dispersal.

IV. SUMMARY AND CONCLUSIONS

In this work we have explored the effect of human mobility on the dynamics of a vector borne infection. We have added this characteristic of human behavior on an already tested model of dengue dispersal when the dynamics is driven by mosquitoes alone. We have analyzed the case of a schematic city of 20 × 20 blocks with 100 individuals per block.

We have considered two temperature profiles: one with a simple constant temperature and one with a realistic time distribution corresponding to the city of Buenos Aires, Argentina.

Another variable in our analysis has been the number of breeding cites in the city; we have considered 50, 100, 200, 300, and 400 breeding cites per block.

Human mobility has been described by superimposing diverse kinds of networks in which links represent the daily movement of humans. The distribution of lengths of these links are derived from recent studies on human motion and in particular, taking into account the finding that human behavior is highly predictable. We have also considered reference patterns, i.e., purely random motion and random motion of a single human per block. We have explored different observables such as size and duration of the outbreaks and complementary morphological characteristics of the pattern of recovered individuals.

From the analysis described above we can conclude that human mobility strongly enhances the infection dispersal. As can be clearly seen from Fig. 7, even for the case in which just one individual per block can perform a long jump, the epidemic spreads over all the "city" very early in the evolution at variance with the case when the epidemic is driven by the mosquitoes alone (Fig. 5). This effect can be traced to the fact that when the disease dispersal is driven by mosquitoes alone we have a single focus that expands due to the diffusive kind of dynamics associated with mosquito dispersal. When human mobility is taken into account, multiple foci appear as the time evolution is followed. Human mobility increases both the size and the speed of propagation of the outbreaks. The increase in speed is particularly relevant when seasonality is present, such as in a city like Buenos Aires, and this is taken into account. Because of the low temperatures reached in winter, the population of mosquitoes is severely reduced, as displayed in Fig. 2, so if the dispersal happens at a slow pace, the reduction in the population of mosquitoes (related to the decrease of the mean temperature) is the responsible for the end of the epidemics. We have found that for the motion patterns associated with the shortest mean path lengths and 400 BS/ha the epidemics can reach all of the population before this reduction. This feature can be captured by the quantity "power of the epidemics" defined as the quotient of the size of the epidemics divided by its time span. This quantity displays a monotonic increase as the mean length path of the networks describing the daily human mobility pattern, decreases. These findings indicate that human mobility might turn out to be the main driving force in the epidemics dynamics. Both in the case of a fixed temperature and that with seasonal variational temperatures, human motion gives rise to faster and more widespread epidemics. Finally, these findings indicate that, when considering

measures to fight epidemics dispersal human motion should be one of the top concerns. We are presently exploring this issue.

ACKNOWLEDGMENTS

We thank the University of Buenos Aires for support through Grant No. X210.

[1] D. J. Gubler, Clin. Microbiol. Rev. **11**, 480 (1998).
[2] WHO, *Dengue and Dengue Hemorrhagic Fever*, Fact sheet N117 (2009) [http://www.who.int/mediacentre/factsheets/fs117/en/index.html].
[3] T. Botari, S. G. Alves, and E. D. Leonel, Phys. Rev. E **83**, 037101 (2011).
[4] E. A. C. Newton and P. Reiter, Am. J. Trop. Med. Hyg. **47**, 709 (1992).
[5] D. A. Focks, D. G. Haile, E. Daniels, and G. A. Mount, J. Med. Entomol. **30**, 1003 (1993).
[6] D. A. Focks, D. G. Haile, E. Daniels, and G. A. Mount, J. Med. Entomol. **30**, 1018 (1993).
[7] D. A. Focks, D. G. Haile, E. Daniels, and D. Keesling, Am. J. Trop. Med. Hyg. **53**, 489 (1995).
[8] M. Otero and H. G. Solari, Math. Biosci. **223**, 32 (2010).
[9] M. Otero, H. G. Solari, and N. Schweigmann, Bull. Math. Biol. **68**, 1945 (2006).
[10] M. Otero, N. Schweigmann, and H. G. Solari, Bull. Math. Biol. **70**, 1297 (2008).
[11] L. Esteva and C. Vargas, Math. Biosci. **150**, 131 (1998).
[12] L. Esteva and C. Vargas, J. Math. Biol. **38**, 220 (1999).
[13] L. Esteva and C. Vargas, Math. Biosci. **167**, 51 (2000).
[14] L. M. Bartley, C. A. Donnelly, and G. P. Garnett, Trans. R. Soc. Trop. Med. Hyg. **96**, 387 (2002).
[15] P. Pongsumpun and I. M. Tang, Math. Comput. Modell. **37**, 949 (2003).
[16] G. Chowell, P. Diaz-Dueñas, J. C. Miller, A. Alcazar-Velazco, J. M. Hyman, P. W. Fenimore, and C. Castillo-Chavez, Math. Biosci. **208**, 571 (2007).
[17] C. Favier, D. Schmit, C. D. M. Müller-Graf, B. Cazelles, N. Degallier, B. Mondet, and M. A. Dubois, Proc. R. Soc. London **272**, 1171 (2005).
[18] M. J. Otero, D. Barmak, C. O. Dorso, H. G. Solari, and M. A. Natiello, doi:10.1016/j.mbs.2011.04.006.
[19] J. M. Epstein, J. Parker, D. Cummings, and R. A. Hammond, PLoS ONE **3**, e3955 (2008).
[20] T. Gross and B. Blasius, J. R. Soc., Interface **5**, 259 (2008).
[21] T. Gross, Carlos J. Dommar D'Lima, and B. Blasius, Phys. Rev. Lett. **96**, 208701 (2006).
[22] S. Risau-Gusmans and D. H. Zanette, J. Theor. Biol. **257**, 52 (2009).
[23] D. H. Zanette, e-print arXiv:0707.1249.
[24] D. H. Zanette and S. R. Gusman, J. Biol. Phys. **34**, 135 (2007).
[25] W. Lig, Y. Jia-Ren, Z. Jian-Guo, and L. Zi-Ran, Chin. Phys. **16**, 2498 (2007).
[26] N. H. Fefferman and K. L. Ng, Phys. Rev. E **76**, 031919 (2007).
[27] S. Funk, M. Salathé, and V. A. A. Jansen, J. R. Soc. Interface **7**, 1247 (2010).
[28] Z. Zhao, J. P. Calderón, C. Xu, G. Zhao, D. Fenn, D. Sornette, R. Crane, P. M. Hui, and N. F. Johnson, Phys. Rev. E **81**, 056107 (2010).
[29] L. Sattenspiel, *The Geographic Spread of Infectious Diseases: Models and Applications* (Princeton University, Princeton, NJ, 2009).
[30] I. Rhee, M. Shin, S. Hong, K. Lee, and S. Chong, Technical Report, Computer Science Department, North Carolina State University, 2007 (unpublished).
[31] M. C. González, C. A. Hidalgo, and A.-L. Barabási, Nature (London) **453**, 779 (2008).
[32] D. Brockmann, L. Hufnagel, and T. Geisel, Nature (London) **439** (2006).
[33] L. H. D. Brockmann, *The Scaling Law of Human Travel—A Message from George* (World Scientific, Singapore, 2007).
[34] G. Chowell, J. M. Hyman, S. Eubank, and C. Castillo-Chavez, Phys. Rev. E **68**, 066102 (2003).
[35] C. Cattuto, W. van den Broeck, A. Barrat, V. Colizza, J.-F. Pinton, and A. Vespignani, PLoS ONE **5**, e11596 (2010).
[36] J. Candia, M. C. González, P. Wang, T. Schoenharl, and A.-L. Barabási, http://arxiv.org/pdf/0710.2939.
[37] P. Wang and M. C. González, Philos. Trans. R. Soc. London, Ser. A **367**, 3321 (2009).
[38] A. Buscarino, L. Fortuna, M. Frasca, and V. Latora, Europhys. Lett. **82**, 38002 (2008).
[39] X. Li, L. Cao, and G. F. Cao, Eur. Phys. J. B **75**, 319 (2010).
[40] M. Keeling and K. T. Eames, J. R. Soc., Interface 22 **2**, 295 (2005).
[41] P. Pongsumpun, D. G. Lopez, C. Favier, L. Torres, J. Llosa, and M. Dubois, Trop. Med. Int. Health **13**, 1180 (2008).
[42] S. T. Stoddard, A. C. Morrison, G. M. Vazquez-Prokopec, V. P. Soldan, T. J. Kochel, U. Ktron, J. P. Elder, and T. W. Scott, PLoS Negl. Trop. Dis. **3**, e481 (2009).
[43] A. Seijo, Y. Romer, M. Espinosa, J. Monroig, S. Giamperetti, D. Ameri, and L. G. Antonelli, Medicina (B Aires) **69**, 593 (2009).
[44] H. Nishiura and S. B. Halstead, J. Infect. Dis. **195**, 1007 (2007).
[45] C. Song, Z. Qu, N. Blumm, and A.-L. Barabási, Science **327**, 1018 (2010).
[46] J. W. Tukey, *Exploratory Data Analysis* (Addison-Wesley, Reading, MA, 1977).